Timing of post-collisional volcanism in the eastern part of the Variscan Belt: constraints from SHRIMP zircon dating of Permian rhyolites in the North-Sudetic Basin (SW Poland)

MAREK AWDANKIEWICZ*, RYSZARD KRYZA & NORBERT SZCZEPARA

University of Wroclaw, Institute of Geological Sciences, ul. Cybulskiego 30, 50-205 Wroclaw, Poland

Abstract – The final stages of the Variscan orogeny in Central Europe were associated with voluminous granitic plutonism and widespread volcanism. Four samples representative of the main rhyolitic volcanic units from the Stephanian–Permian continental succession of the North-Sudetic Basin, in the eastern part of the Variscan Belt, were dated using the SIMS (SHRIMP) zircon method. Three samples show overlapping ^{206}Pb–^{238}U mean ages of 294 ± 3, 293 ± 2 and 292 ± 2 Ma, and constrain the age of the rhyolitic volcanism in the North-Sudetic Basin at 294–292 Ma. This age corresponds to the Early Permian – Sakmarian Stage and is consistent with the stratigraphic position of the lava units. The fourth sample dated at 288 ± 4 Ma reflects a minor, younger stage of (sub)volcanic activity in the Artinskian. The silicic activity was shortly followed by mafic volcanism. The rhyolite samples contained very few inherited zircons, possibly owing to limited contribution of crustal sources to the silicic magma, or owing to processes involved in anatectic melting and magma differentiation (e.g. resorption of old zircon by Zr-undersaturated melts). The SHRIMP results and the stratigraphic evidence suggest that the bimodal volcanism terminated the early, short-lived (10–15 Ma) and vigorous stage of basin evolution. The Permian volcanism in the North-Sudetic Basin may be correlated with relatively late phases of the regional climax of Late Palaeozoic volcanism in Central Europe, constrained by 41 published SHRIMP zircon age determinations at 299–291 Ma. The Permian volcanism and coeval plutonism in the NE part of the Bohemian Massif can be linked to late Variscan, post-collisional extension.

Keywords: Variscan volcanism, Variscan orogeny, Central European Variscides, SHRIMP zircon dating.

1. Introduction

The collision of continental plates in Late Palaeozoic times led to the Variscan and Alleghanian orogeny and to the assembly of the Pangaea supercontinent. The final stages of the collisional and orogenic processes were associated with, and followed by, voluminous granitic plutonism as well as widespread volcanic activity (e.g. Kryza, Mazur & Oberc-Dziedzic, 2004; Ziegler & Dezes, 2006; Mazur *et al.* 2006, 2007; McCann & Kiersnowski, 2008; Timmerman, 2008; Oberc-Dziedzic *et al.* 2013*a, b*). This late- to post-orogenic, large-scale magmatism is genetically linked with extension-related mantle melting (including subduction-modified mantle sources), crustal anatexis and variable differentiation and interaction of mantle and crustal melts. The granitic plutons, sealing active tectonic zones and young sutures, as well as volcanic suites, filling extensional troughs, significantly contributed to the formation and consolidation of the newly generated continental crust. Large volumes of silicic lavas and ignimbrites influenced the palaeoenvironment by changing topography and sedimentation patterns (Geißler, Breitkreuz & Kiersnowski, 2008) and

volcanic gases possibly contributed to climate cooling (Cather *et al.* 2009).

Critical constraints for geodynamic and petrological models of the Carboniferous to Permian magmatism as well as its palaeoenvironmental significance include age determinations and correlations of various igneous suites across the collisional belt. The Sudetes, located in the eastern part of the Central European Variscides, in a zone strongly affected by regional strike-slip dislocations, expose numerous granitic plutons cropping out in uplifted basement blocks, as well as coeval volcanic suites preserved in the intervening Late Palaeozoic troughs (Fig. 1). In recent years, increasing amounts of new age determinations of the granites, including SHRIMP (sensitive high-resolution ion microprobe) zircon ages, provided more precise data on the Late Palaeozoic evolution of plutonism in the region (Awdankiewicz *et al.* 2010*a*; Oberc-Dziedzic, Kryza & Białek, 2010; Kryza *et al.* 2012; Oberc-Dziedzic & Kryza, 2012; Oberc-Dziedzic *et al.* 2013*a, b*). However, the Permo-Carboniferous volcanic successions have remained largely undated, hindering more precise correlations both with granites and with similar volcanic suites in the neighbouring segments of the Variscan orogenic belt.

This study is focused on the North-Sudetic Basin, a Late Palaeozoic trough hosting a continental

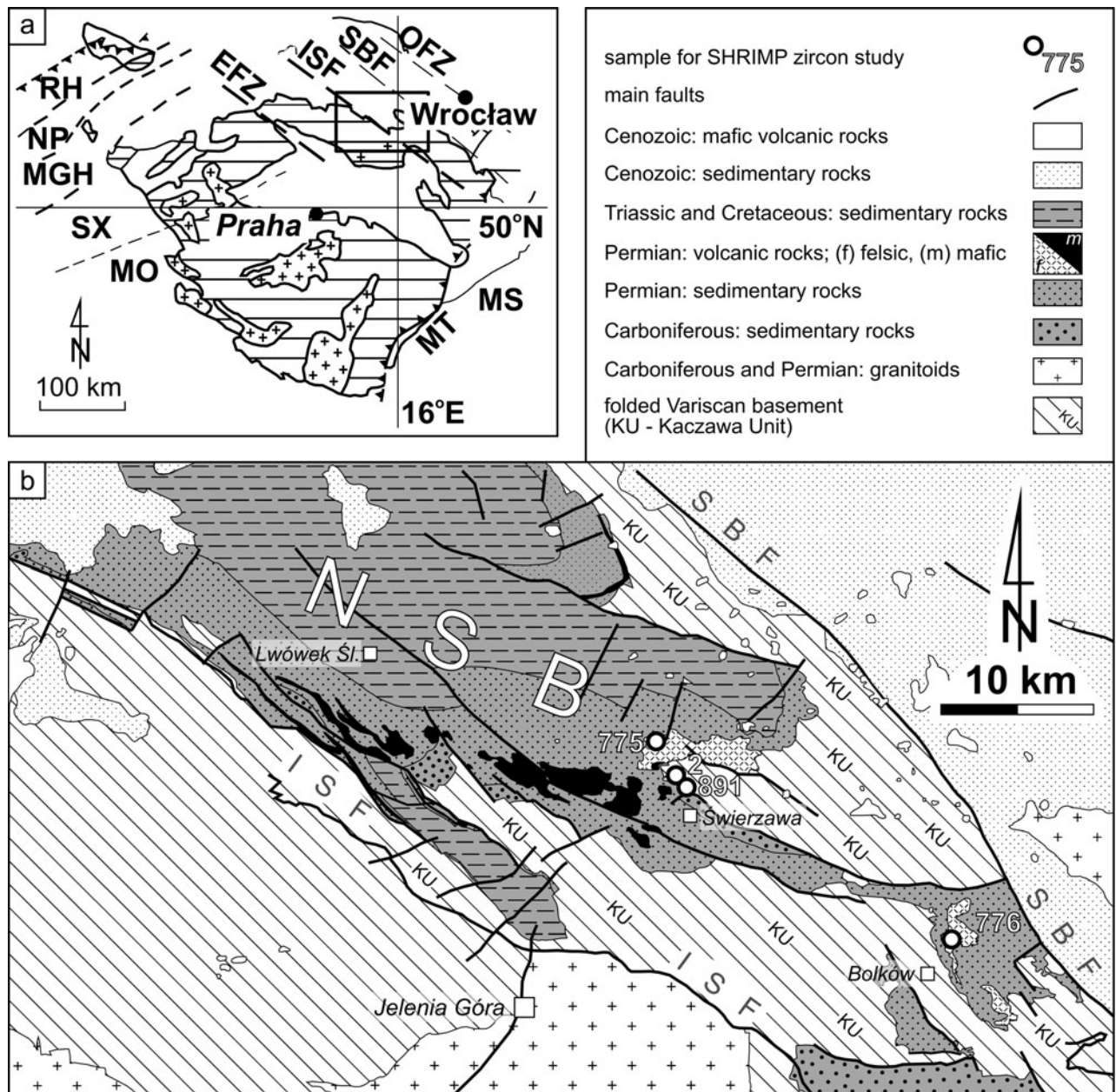*Author for correspondence: marek.awdankiewicz@ing.uni.wroc.pl

Figure 1. (a) Location of the study area (frame) in the Bohemian Massif in the eastern part of the Variscan Belt of Europe. EFZ – Elbe Fault Zone; ISF – Intra-Sudetic Fault; MGH – Mid-German High; MO – Moldanubian Zone; MS – Moravo-Silesian Zone; MT – Moldanubian Thrust; NP – Northern Phyllite Zone; OFZ – Odra Fault Zone; RH – Rheno-Hercynian Zone; SBF – Sudetic Boundary Fault; SX – Saxo-Thuringian Zone. Large Variscan granitoid plutons indicated with crosses. (b) Geological sketch map of the North-Sudetic Basin (NSB) and adjacent areas (modified from Bossowski, Sawicki & Wroński, 1981; Milewicz, Szałamacha & Szałamacha, 1989). Sampling sites for SHRIMP zircon dating are indicated (for coordinates see Table 1).

volcano-sedimentary succession with an interstratified bimodal volcanic suite. A modified lithostratigraphic scheme of this volcano-sedimentary succession is proposed. Using rhyolites for SHRIMP zircon dating, we put constraints on the timing of volcanism in the basin. The geochronological and stratigraphic evidence provides insights into the interrelationships between tectonic, volcanic and depositional processes during the evolution of the basin. The age of the bimodal volcanic suite of the North-Sudetic Basin is discussed within the context of already published SHRIMP ages of Permian volcanic rocks in Central Europe.

2. Outline of geology

2.a. The Sudetes and the North-Sudetic Basin

The Sudetes are located in the eastern part of the Variscan Belt of Europe, at the northeastern margin of the Bohemian Massif (Fig. 1a). The Variscan orogeny formed the crustal basement, and the late- to post-orogenic tectonic activity, volcanism and contemporaneous vivid erosion and sedimentation shaped the surface mosaic structure of that area (Kryza, Mazur & Oberc-Dziedzic, 2004; Mazur et al. 2006). The Variscan orogenic processes were diachronous,

initiated in some units in the Mid–Late Devonian, and considerably later, around the Early–Late Carboniferous boundary, in other areas. The intense magmatism, including vast granitoid plutonism and bimodal volcanism, occurred in a broad time span, between around 340 and 280 Ma (e.g. Mazur *et al.* 2007), with major events, documented by SHRIMP zircon dating of granitoids, at ~ 340, 328, 312, 305–300 and 295–280 Ma (Oberc-Dziedzic, Kryza & Białek, 2010; Kryza *et al.* 2012; Oberc-Dziedzic & Kryza, 2012; Oberc-Dziedzic *et al.* 2013*a*, *b* and references therein). The onset of intense late-orogenic sedimentation in intramontane basins in this region is dated by biostratigraphic evidence between the Viséan (in the Intra-Sudetic Basin; Turnau, Żelaźniewicz & Franke, 2002) and Stephanian (in the North-Sudetic Basin; Milewicz & Górecka, 1965; Górecka, 1970). The mosaic of the basement units in this part of the Bohemian Massif was significantly modified by large-scale strike-slip displacements (Aleksandrowski *et al.* 1997).

The North-Sudetic Basin, one of the major post-orogenic basins of that area, is confined between two major fault zones, the Sudetic Boundary Fault in the north and the Intra-Sudetic Fault in the south (Fig. 1). The basin is a WNW-trending depression, with a system of grabens and horsts in the southern and eastern parts. The basin fill comprises the uppermost Carboniferous to Upper Cretaceous deposits, with a major hiatus spanning the Upper Triassic, Jurassic and Lower Cretaceous. The lower part of the basin fill (Upper Carboniferous – Lower Permian) is a continental, volcano-sedimentary succession of, mainly, siliciclastic deposits. The upper part (Upper Permian – Zechstein, Lower Triassic, Upper Cretaceous) comprises various siliciclastic and carbonate deposits as well as evaporites of shallow marine, epicontinental and, partly, continental origin. The maximum total thickness of the basin fill reaches *c.* 4 km and the mean thickness is *c.* 2 km (Milewicz, 1968; Baranowski *et al.* 1990). The North-Sudetic Basin originated as a late Variscan intramontane trough, related to extensional and wrench tectonics during the late stages of the Variscan orogeny (cf. McCann *et al.* 2006). On a broader scale, the development of the North-Sudetic Basin can also be linked with the evolution of the southeastern part of the extensive Permo-Mesozoic Central European Basin System (Scheck-Wenderoth & Lamarche, 2005; Ziegler & Dezes, 2006).

The basement of the North-Sudetic Basin comprises low-grade metamorphic rocks which belong to the Kaczawa Unit (Fig. 1). The latter, together with neighbouring tectonostratigraphic units of the West Sudetes, are considered a part of the Armorican Terrane Assemblage of the Variscan Belt (Mazur *et al.* 2006 and references therein). The Kaczawa Complex is interpreted as a fragment of the Variscan accretionary prism and comprises metasedimentary and metavolcanic rocks with Cambrian to Viséan protolith ages (Baranowski *et al.* 1990; Kryza & Zalasiewicz, 2008). These rocks underwent deformation

and metamorphism, mostly at blueschist to greenschist facies and, locally, at very low-grade metamorphic conditions (Kryza *et al.* 2011), during the Variscan orogeny, between the Late Devonian and the Early Carboniferous. Thus, the hiatus between the North-Sudetic Basin fill and its basement rocks spans, roughly, 20 Ma.

Seismic studies show that the rocks of the Kaczawa Complex make up the uppermost 4–5 km of *c.* 33–35 km thick Earth's crust of the region. Petrological and SHRIMP studies of a gneiss xenolith in Cenozoic basanite lava erupted through the Kaczawa Complex suggest that the deeper part of the upper crust of that region contains gneisses similar to those exposed in the Góry Sowie Block to the SE (Oberc-Dziedzic, Kryza & Pin, 2009). The structurally complex middle to lower crustal levels are presumably composed of various crystalline complexes of the Variscan orogenic wedge (Grad *et al.* 2008 and references therein).

2.b. The Permo-Carboniferous volcano-sedimentary succession of the North-Sudetic Basin

The Permo-Carboniferous volcano-sedimentary succession of the North-Sudetic Basin crops out along the southern and eastern margins of the basin (Fig. 1b). This succession is mainly composed of siliciclastic sedimentary rocks: conglomerates, sandstones and shales, forming four fining-upwards cyclothems, each 300–500 m thick. The three lower, more complete, cyclothems begin with coarse-grained alluvial fan and alluvial sediments and end with fine-grained lacustrine deposits. The fourth cyclothem is mainly made up of sandstones. A major unconformity occurs between the third and fourth cyclothems. These continental deposits, included in the Rotliegendes in the classical subdivision of Central European Permian, are overlain by marine deposits related to the Zechstein transgression (Kozłowski & Parachoniak, 1967; Wojewoda & Mastalerz, 1989; Baranowski *et al.* 1990; Mastalerz, 1990).

According to Wojewoda & Mastalerz (1989), Mastalerz (1990) and Wagner (2008), the Permo-Carboniferous succession comprises the Świerzawa, Wielisławka and Bolesławiec formations assigned to the Stephanian – Lower Autunian, Upper Autunian and Saxonian, respectively. Sporomorph assemblages document the age of the lowermost members of the basin fill as Stephanian A–C (Milewicz & Górecka, 1965; Górecka, 1970), which corresponds to the Kasimovian–Gzhelian stages of the Upper Pennsylvanian in the international chronostratigraphic subdivision (ICS, 2012). The Wielisławka Formation is correlated with the Sakmarian Stage, and the Bolesławiec Formation together with the overlying marine Zechstein deposits, is assigned to the Upper Permian – Wuchiapingian Stage (Wagner, 2008; Peryt, 1978 and references therein). Thus, the accumulation of the Świerzawa,

Wielisławka and Bolesławiec formations spanned some 50 Ma, including a hiatus of *c.* 30 Ma between the Wielisławka and Bolesławiec formations.

The Świerzawa Formation, at the base of the basin fill, contains intercalations of tuffaceous sandstones and pebbles of volcanic rocks (Ostromęcki, 1972), possibly indicative of some volcanic activity during the initial phases of basin evolution, or erosion of some older volcanic deposits. However, intercalations of volcanic rocks, a few hundred metres thick, are characteristic of the upper part of the overlying Wielisławka Formation. These Permian volcanic rocks represent a bimodal, mafic-felsic suite with a strong lateral variation of rock assemblages. Mafic rocks are widespread in the west, felsic and less common mafic rocks occur in the central part, and solely felsic rocks occur in the east (Fig. 1b). The mafic volcanic rocks are mainly basaltic andesites and basaltic trachyandesites, which were erupted from fissures and/or small shield volcanoes as lava flows and locally also emplaced as shallow-level subvolcanic intrusions (Milewicz, 1965; Kozłowski & Parachoniak, 1967; Awdankiewicz, 2006). The felsic rocks are rhyolites that occur as lava flows, shallow-level intrusive to extrusive bodies, tuffs and other volcaniclastic deposits, as well as minor dykes (Kozłowski & Parachoniak, 1967; Skurzewski, 1981; M. Pańczyk, unpub. PhD thesis, Warsaw Univ., 2003; Szczepara & Awdankiewicz, 2010; Awdankiewicz *et al.* 2010b; Szczepara, 2012).

According to Kozłowski & Parachoniak (1967), the 'Rotliegendes eruptive complex' originated in two cycles: in each cycle, mafic lavas were followed by felsic lavas or tuffs. However, as discussed by Awdankiewicz (2006), this concept must be treated with caution, because:

(1) volcanic rocks of the 'first cycle' comprise small outcrops of very limited extent, being rather related to small-scale and local (sub)volcanic events and not to a basin-scale stage of activity;

(2) a vast majority of volcanic rocks belongs to the 'second cycle';

(3) north of the town of Świerzawa, near the centre of the basin, in the key area where mafic and felsic rocks of the 'second cycle' occur in close association, the emplacement sequence was the opposite to that proposed by Kozłowski & Parachoniak (1967) – the mafic rocks form subvolcanic intrusions that are younger than the associated felsic volcanics.

Tentative lithostratigraphic subdivisions of the volcano-sedimentary succession in the central and eastern parts of the basin are shown in Figure 2. They are partly based on the scheme proposed by Wojewoda & Mastalerz (1989), but they highlight, in more detail, the relationships between the volcanic rocks, incorporating data from published papers and detailed geological maps (Frąckiewicz, 1958; Milewicz, 1965; Kozłowski & Parachoniak, 1967; Skurzewski, 1981; Milewicz & Kozdrój, 1995), as well as the observations outlined above. The felsic volcanic rocks, which are the main subject of this paper, are further subdivided into a few

smaller units, each characterized by a specific geological position, lithology and structure: the Wielisławka, Sędziszowa, Różana and Bolków rhyolites.

The Wielisławka Rhyolites crop out in the NW part of a horst (the Świerzawa Horst), mainly within the uplifted Lower Palaeozoic metasedimentary rocks of the Kaczawa Complex, but are also in contact (intrusive or tectonic?) with the Lower Autunian deposits in the west. The main lithology is a porphyritic rhyolite, characterized by flow foliation and spectacular columnar joints which define concentric and radial patterns, respectively. Rhyolitic breccias occur in the eastern part of the outcrop (Szczepara, unpub. data). The Wielisławka Rhyolites are interpreted as a subvolcanic intrusion (Jerzmański, 1956; Kozłowski & Parachoniak, 1967 and references therein) or a remnant/root of a lava dome (Awdankiewicz *et al.* 2010b).

The Sędziszowa Rhyolites comprise a group of small dykes cutting the basement rocks in the Świerzawa Horst south and east of the Wielisławka Rhyolites. According to a cross-section by Zimmermann & Kuhn (1918), some of these dykes may project from the Wielisławka Rhyolites. Other dykes, however, are distributed over larger distances from the Wielisławka Rhyolites and are spatially unrelated.

The Różana Rhyolites represent the largest outcrop of silicic rocks in the North-Sudetic Basin, *c.* 8 × 3 km in size. These rhyolites occur within Lower Autunian deposits along the northern margin of the Świerzawa Horst, partly in tectonic contact with the latter, and are overlain by Saxonian deposits. Porphyritic, massive rhyolites predominate, but rhyolitic breccias and other volcaniclastic deposits are also found. Spherulitic rhyolites, lithophysae and agates are locally abundant. The Różana Rhyolites can be interpreted as a partly eroded lava flow, or a complex of lava flows (Kozłowski & Parachoniak, 1967; Awdankiewicz *et al.* 2010b; Szczepara, 2012). Near the base of this unit, adjacent to the Świerzawa Horst, mafic volcanic rocks occur as sills/laccoliths with peperitic margins and, further SW, mafic lavas as well as subvolcanic intrusions are found (Awdankiewicz, 2006).

The Bolków Rhyolites crop out in the easternmost part of the North-Sudetic Basin in a local basin known as the Wolbromek Trough. The Bolków Rhyolites are intercalated in the Lower Autunian sediments and overlain by Saxonian deposits. The main outcrop is a porphyritic, predominantly coherent rhyolite, 100–200 m thick; there are also associated thin veins in adjacent Autunian deposits. To the south and east, *c.* 10–20 m thick rhyolitic tuffs occur at an equivalent stratigraphic position. Skurzewski (1981) considered the main rhyolite body as a partly eroded extrusion or subvolcanic intrusion, possibly composed of a few smaller units. However, M. Pańczyk (unpub. Ph.D. thesis, Warsaw Univ., 2003) suggested that the rhyolites comprise lavas as well as extremely welded, high-grade ignimbrites.

Limited dating work on the volcanic rocks of the North-Sudetic Basin has been carried out so far.
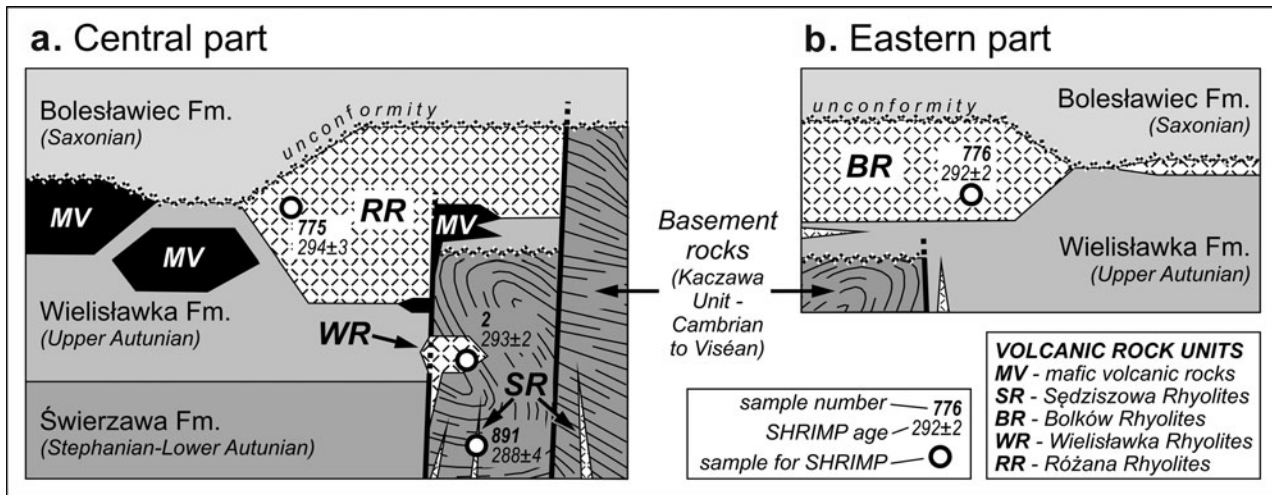
Figure 2. Tentative lithostratigraphy of the volcano-sedimentary succession studied: (a) central part, (b) eastern part of the North-Sudetic Basin.

Pańczyk & Bachliński (2004), using the Rb–Sr isochron method, suggested that the emplacement of the rhyolites took place at *c.* 260 Ma. However, this 'age' is apparently too young compared with the stratigraphic position of the volcanic rocks and may rather reflect some disturbance of the Rb–Sr isotopic system, e.g. owing to post-magmatic alteration or some isotopic heterogeneity of the samples. Pękala, Wójtowicz & Michalik (2003) dated celadonite from amygdales in altered mafic lavas from Lubiechowa using the K–Ar method. They suggested that the alteration of these rocks spanned a prolonged period of time from 252.5 to 177.5 Ma (Late Permian to Middle Jurassic).

3. Methods

Initially, ten samples of the mafic and felsic volcanic rocks representative of the main eruptive units within the basin were collected for the SHRIMP study. The samples, about 1–3 kg in weight, were crushed and sieved, and the 0.063–0.25 mm heavy fraction separated using the conventional heavy liquid (sodium polytungstate) procedure. Six samples of mafic rocks turned out to be zircon free and thus excluded from further work. Four samples of rhyolites yielded abundant zircons; hand-picked crystals representing various morphological types were mounted in epoxy resin, and the polished sections were used for optical microscopy, cathodoluminescence (CL) imaging and SHRIMP analysis.

The zircons were analysed by means of the Sensitive High-Resolution Ion Microprobe (SHRIMP II) in the Beijing SHRIMP Centre, Chinese Academy of Geological Sciences. The SHRIMP U–Pb analyses were performed by applying a secondary electron multiplier in peak-jumping mode following the procedure described in Williams (1998). A primary beam of molecular oxygen was employed to bombard zircon in order to sputter secondary ions. The elliptical analytical spots had a

size of *c.* 25×30 μm, and the corresponding ion current was *c.* 4 nA. The sputtered secondary ions were extracted at 10 kV. A 80 μm wide slit of the secondary ion source, in combination with a 100 μm multiplier slit, allowed mass-resolution of $M/\Delta M \geq 5000$ (1 % valley) so that all the possible isobaric interferences were resolved. Two-minute rastering was employed before each analysis in order to remove the gold coating and possible surface common Pb contamination.

The following ion species were measured in sequence: $^{196}(Zr_2O)$–^{204}Pb–background (*c.* 204 AMU)–^{206}Pb–^{207}Pb–^{208}Pb–^{238}U–^{248}ThO–^{254}UO with an integration time ranging from 2 to 20 seconds. Four cycles for each spot were acquired. Each fifth measurement was carried out on the zircon Pb–U standard TEMORA 1 (Black *et al.* 2003) with an accepted ^{206}Pb–^{238}U age of 416.75 ± 0.24 Ma. The 91500 zircon with a U concentration of 81.2 ppm and a ^{206}Pb–^{238}U age of 1062.4 ± 0.4 Ma (Wiedenbeck *et al.* 1995) was applied as a 'U-concentration' standard.

The collected data were then processed with the SQUID v1.12 (Ludwig, 2005*a*) and ISOPLOT/Ex 3.22 (Ludwig, 2005*b*) software, using the decay constants of Steiger & Jäger (1977). The common Pb correction was done using measured ^{204}Pb according to the model of Stacey & Kramers (1975). The ages given in the text, if not additionally specified, are ^{206}Pb–^{238}U dates. The errors in the text and tables are at the 1σ level for individual points, and at the 2σ level in Concordia diagrams.

4. Results

4.a. Sample characteristics

The location of sampling sites for our SHRIMP study, together with the coordinates and sample characteristics, are given in Figure 1 and Table 1. Sample 2 was collected in the western part of the Wielisławka Rhyolites, in a locally well-known 'Organy Wielisławskie'

Table 1. Lithofacial and petrographic characteristics of the rhyolite samples dated by the SHRIMP method. Coordinates of the sampling sites are given.

	Sample		Phenocrysts			Groundmass		
No	Volcanic unit [coordinates of sampling site]	Lithofacies	Content [%]	Size: *mean; max.* [mm]	Minerals	Texture	Minerals	Comments
2	Wielisławka Rhyolites, [51° 2′ 4.40″ N, 15°52′ 10.12″ E]	columnar-jointed, flow-foliated, coherent, porphyritic rhyolite	10–15	∼ 0.6; 3	Kfs, Qtz, Pl*, Bt*, Opq	finely laminated, microcrystalline, felsitic	Afs, Qtz, Opq	Pl* – albite and kaolinite pseudomorphs after plagioclase; Bt* – biotite partly replaced by chlorite and opaques
775	Różana Rhyolites, [51° 3′ 26.08″ N, 15° 51′ 41.90″ E]	massive, coherent, porphyritic rhyolite	20–25	∼ 1; 4	Kfs, Pl*, Qtz, Bt*, Opq	microcrystalline, felsitic with isolated spherulites	Afs, Qtz, Opq	Pl* – kaolinite pseudomorphs after plagioclase; Bt* – opaque pseudomorphs after biotite
776	Bolków Rhyolites, [50° 56′ 16.1″ N, 16° 6′ 47.9″ E]	platy-jointed. coherent, porphyritic rhyolite	20–25	∼ 1.2; 5	Kfs, Pl*, Qtz, Bt*, Opq	microcrystalline, finely laminated, trachytic (aligned microliths)	Afs, Qtz, Pl*, Maf*, Opq	Bt* – opaque pseudomorphs after biotite; Maf* – opaque pseudomorphs after biotite and other Fe-Mg minerals; Pl* – albitized plagioclase
891	Sędziszowa Rhyolites, [51° 1′ 44.74″ N, 15° 52′ 37.79″ E]	massive, coherent, porphyritic rhyolite	10–15	∼ 1; 4.5	Fsp*, Qtz, Bt*, Opq	microcrystalline, felsitic to micropoikilitic (Qtz with Afs inclusions)	Qtz, Afs, Opq	Fsp* – kaolinite pseudomorphs after feldspars, brownish staining by Fe hydroxides; Bt* – kaolinite and opaque pseudomorphs after biotite

Afs – alkali feldspar; Bt – biotite; Kfs – K-feldspar; Opq – opaque minerals; Qtz – quartz.

quarry, protected as a nature monument because a spectacular system of columnar joints is well exposed there. Sample 891 of the Sędziszowa Rhyolites comes from a small, strongly overgrown quarry in a dyke, south of 'Organy Wielisławskie'. Sample 775 represents the Różana Rhyolites and was collected in the northwestern, upper part of this unit, near the base of a *c*. 15 m high cliff where coherent rhyolites interdigitate with autoclastic rhyolitic breccias. Sample 776 is the Bolków Rhyolite from the southern part of the main rhyolite outcrop, from a *c*. 15 m high cliff exposing massive to platy-jointed rhyolites.

The four samples selected for the SHRIMP study (Table 1) share several main petrographic characteristics, such as modal composition (mainly alkali feldspars, quartz and plagioclase, less abundant biotite and opaques), porphyritic texture (phenocrysts of the same phases as above), microcrystalline groundmass, and significant post-magmatic alteration. The latter includes the replacement of plagioclase by albite and/or kaolinite, replacement of biotite by chlorite, opaques and/or kaolinite, as well as veinlets and streaks of quartz with kaolinite, and abundant pigment of iron oxides/hydroxides in the groundmass. The differences between the samples are relatively small and are mainly in the content and size of phenocrysts, groundmass textures and the degree of replacement of primary igneous phases by post-magmatic minerals.

4.b. Zircon characteristics

The main characteristics of zircon crystals are quite similar in all four samples studied (Fig. 3). The crystals are mostly normal-prismatic, euhedral, rarely subhedral or rounded; quite a lot are broken, which possibly occurred during separation (e.g. sample 2, grains 6.1, 6.2; sample 775, grain 1.1; sample 776, grain 1.1; sample 891, grain 4.1). Small vacuoles, and less frequently other inclusions, are found in many crystals (sample 776, grains 1.1, 2.1). Some zircons are relatively dark in transmitted light owing to abundant cracks and rusty patches, but several grains are clearer and free of these defects. In CL images, the zircons display variable brightness and often distinct, recurrent, concentric 'magmatic' zonation (sample 2, grains 4.2, 8.2, 10.2; sample 775, grain 1.1; sample 776, grains 1.1, 4.1; sample 891, grains 2.1, 6.1, 11.1). Patches and sectors of various CL brightness are less common (sample 2, grain 5.1; sample 775, grains 2.2, 3.2, 6.1; sample 776, grain 6.1). Homogeneous crystals (sample 2, grain 11.1; sample 776, grains 3.1, 12.1; sample 891, grains 1.1, 15.1), as well as those with distinct cores (sample 2, grains 1.1, 9.1; sample 891, grain 7.1) are rare.

4.c. SHRIMP zircon study

CL images of the analysed zircons with the location of analytical spots are shown in Figure 3. The spots were mainly located within the oscillatory zoned margins of crystals in order to determine the magmatic age of the crystals and the emplacement age of the host rhyolites. Some spots were also placed in the central parts of the crystals to check the presence of inherited components. The SHRIMP data are given in Table 2. The Concordia diagrams are shown in Figure 4.

4.c.1. Sample 2 (Wielisławka rhyolite)

In sample 2, 19 spots in 12 crystals were analysed. U and Th contents in 15 spots are low to moderate, between 115 and 572 ppm, and between 87 and 205 ppm, respectively. Three other spots show higher abundances of U (around 1000 ppm) and Th (*c*. 600 ppm), and one outlier (grain 5.1) is very rich in these elements: *c*. 2800 ppm and 1800 ppm, respectively. The $^{206}Pb_c$ is mostly below 1%, and only in the U–Th-rich outlier is extremely high, 29.89%. This outlier point, representing a CL-dark rim of a crystal, is strongly discordant and has been excluded from the mean age calculation. Otherwise, the ^{206}Pb–^{238}U ages reveal a single coherent group of 18 analytical points, lacking any significant inheritance and with a mean ^{206}Pb–^{238}U age (Fig. 4a) of 292.8 ± 2.1 Ma (1σ). This age corresponds to the Early Permian – Sakmarian and likely represents the magmatic crystallization age of the main zircon population in the sample studied, and the emplacement age of the Wielisławka Rhyolites.

4.c.2. Sample 775 (Różana rhyolite)

The data for sample 775 represent 18 spots in 13 crystals. U and Th contents range rather widely, between *c*. 100–1000 ppm and *c*. 40–640 ppm, respectively. The $^{206}Pb_c$ is mostly below 1.80%, except for single spot 9.1. This grain is very dark in the CL image, and shows extremely high U (6847 ppm) and Th (10 508 ppm), and very high $^{206}Pb_c$ of 26.01%. This analytical spot has been excluded from further interpretation. One grain, 8.1, is clearly inherited, having the ^{207}Pb–^{206}Pb age of 1511 ± 23 Ma. Excluding this inherited grain and three other outliers (6.1, 9.1 and 10.2), the remaining 14 spots yield a mean ^{206}Pb–^{238}U age of 294.1 ± 3.1 Ma (Fig. 4b; Early Permian – Sakmarian), which can be interpreted as the crystallization age of the zircons and the emplacement age of the Różana Rhyolites.

4.c.3. Sample 776 (Bolków rhyolite)

In sample 776, 16 spots in 12 crystals were analysed. The U contents range rather widely, from 100 to 855 ppm, whereas the $^{206}Pb_c$ is mostly below 1.71%, except for point 4.1 with an elevated value of 7.12%. The $^{232}Th/^{238}U$ ratios and ^{206}Pb–^{238}U ages are much more homogeneous, i.e. within the range 0.30–0.81 and 285 to 302 Ma, respectively. The mean ^{207}Pb–^{206}Pb age

Figure 3. Pairs of optical photomicrographs (left) and cathodoluminescence images (right) of zircons with location of analytical points. (a) Sample 2. (b) Sample 775. (c) Sample 776. (d) Sample 891. ^{206}Pb–^{238}U ages and 1σ errors are given.

Table 2a. SHRIMP data for rhyolite sample 2

Spot	$^{206}Pb_c$ %	U ppm	Th ppm	$^{232}Th/$ ^{238}U	$^{206}Pb^*$ ppm	Total $^{238}U/$ ^{206}Pb	±%	Total $^{207}Pb/$ ^{206}Pb	±%	(1) $^{207}Pb^*/$ $^{206}Pb^*$	±%	(1) $^{207}Pb^*/$ ^{235}U	±%	(1) $^{206}Pb^*/$ ^{238}U	±%	Err. corr.	(1) $^{206}Pb–^{238}U$ age	(1) $^{207}Pb–^{206}Pb$ age	% Discord-ance
2_1.1	0.28	497	192	0.40	20.2	21.11	1.5	0.0533	2.1	0.0510	2.3	0.3325	2.7	0.04724	1.5	0.550	297.6±4.4	243±53	−23
2_1.2	1.82	572	120	0.22	23.3	21.04	1.5	0.0536	1.9	0.0536	1.9	0.3512	2.4	0.04752	1.5	0.614	299.3±4.3	354±43	16
2_2.1	0.16	336	113	0.35	13.5	21.36	1.6	0.0511	2.6	0.0499	2.9	0.3210	3.3	0.04674	1.6	0.485	294.5±4.6	188±67	−57
2_3.1	0.10	1137	597	0.54	44.6	21.91	1.4	0.05224	1.4	0.0514	1.8	0.3231	2.3	0.04559	1.4	0.616	287.4±4.0	259±42	−11
2_4.1	0.417	418	164	0.41	16.6	21.60	1.6	0.0558	2.3	0.0524	3.8	0.3330	4.1	0.04610	1.6	0.382	290.5±4.4	305±86	5
2_4.2	1.83	461	136	0.30	18.4	21.50	1.5	0.0515	2.2	0.0515	2.2	0.3305	2.7	0.04652	1.5	0.569	293.1±4.4	265±50	−11
2_5.1	29.89	2752	1763	0.66	70.9	33.37	1.4	0.3643	0.5	0.1600	13.0	0.4620	14.0	0.02101	3.3	0.242	134.0±4.4	2542±220	95
2_6.1	1.03	467	171	0.38	18.8	21.31	1.6	0.0630	2.8	0.0548	6.8	0.3510	7.0	0.04645	1.6	0.233	292.7±4.6	403±150	27
2_6.2	0.68	221	95	0.44	8.9	21.31	1.7	0.0535	3.2	0.0480	4.3	0.3090	4.7	0.04662	1.7	0.368	293.7±4.9	100±100	−193
2_7.1	0.29	482	205	0.44	19.6	21.18	1.6	0.0546	2.1	0.0523	2.7	0.3390	3.1	0.04708	1.6	0.498	296.5±4.5	296±62	0
2_7.2	0.36	875	623	0.74	34.7	21.68	1.4	0.0546	1.6	0.0517	1.9	0.3279	2.4	0.04597	1.4	0.608	289.7±4.1	274±43	−6
2_8.1	0.78	290	108	0.38	11.4	21.89	1.6	0.0573	2.8	0.0510	5.1	0.3190	5.4	0.04532	1.7	0.310	285.7±4.7	242±120	−18
2_8.2	0.44	186	151	0.84	7.5	21.41	1.9	0.0525	3.4	0.0490	5.0	0.3140	5.3	0.04651	1.9	0.353	293.0±5.4	147±120	−100
2_9.1	0.76	342	87	0.26	14.2	20.72	1.6	0.0573	2.3	0.0512	5.0	0.3380	5.3	0.04789	1.6	0.301	301.6±4.7	250±120	−20
2_9.2	0.23	469	114	0.25	18.8	21.40	1.5	0.0541	2.4	0.0523	2.8	0.3360	3.2	0.04662	1.5	0.473	293.8±4.4	297±65	1
2_10.1	0.13	412	393	0.99	16.3	21.64	1.8	0.0556	2.2	0.0546	2.7	0.3470	3.2	0.04615	1.8	0.556	290.8±5.1	395±60	26
2_10.2	0.26	432	203	0.48	17.3	21.50	1.5	0.0560	2.2	0.0540	2.4	0.3452	2.9	0.04639	1.5	0.530	292.3±4.4	370±55	21
2_11.1	0.08	1208	521	0.45	48.1	21.59	1.4	0.0540	1.3	0.0533	1.5	0.3402	2.1	0.04627	1.4	0.680	291.6±4.0	342±34	15
2_12.1	0.70	115	90	0.81	4.5	22.00	2.0	0.0626	4.1	0.0570	4.9	0.3550	5.3	0.04513	2.0	0.387	284.5±5.7	490±110	42

Errors are 1-sigma; Pb_c and Pb^* indicate the common and radiogenic portions, respectively.
Error in Standard calibration was 0.49 % (not included in the above-mentioned errors but required when comparing data from different mounts).
(1) Common Pb corrected using measured ^{204}Pb.

Table 2b. SHRIMP data for rhyolite sample 775

Spot	$^{206}Pb_c$ %	U ppm	Th ppm	$^{232}Th/^{238}U$	$^{206}Pb^*$ ppm	Total $^{238}U/^{206}Pb$	±%	Total $^{207}Pb/^{206}Pb$	±%	(1) $^{207}Pb^*/^{206}Pb^*$	±%	(1) $^{207}Pb^*/^{235}U$	±%	(1) $^{206}Pb^*/^{238}U$	±%	Err. corr.	(1) ^{206}Pb–^{238}U age	(1) ^{207}Pb–^{206}Pb age	% Discord-ance
775_1.1	0.00	146	69	0.49	6.0	20.88	1.9	0.0562	3.8	0.0562	3.8	0.3710	4.2	0.04789	1.9	0.445	301.6±5.5	459±83	34
775_2.1	0.61	1010	289	0.30	39.8	21.77	1.4	0.0581	1.4	0.0532	2.7	0.3350	3.1	0.04566	1.4	0.473	287.8±4.1	336±61	14
775_2.2	0.12	986	398	0.42	38.8	21.85	1.7	0.0526	1.6	0.0517	1.8	0.3257	2.5	0.04572	1.7	0.690	288.2±4.9	271±42	− 6
775_3.1	0.25	707	380	0.56	28.4	21.39	1.5	0.0529	1.7	0.0510	2.5	0.3276	2.9	0.04663	1.5	0.506	293.8±4.2	239±57	− 23
775_3.2	0.14	452	153	0.35	18.5	20.97	1.8	0.0524	2.2	0.0513	2.4	0.3369	3.0	0.04763	1.8	0.596	299.9±5.2	255±55	− 18
775_4.1	0.46	195	70	0.37	7.8	21.50	1.7	0.0559	3.2	0.0522	4.9	0.3330	5.2	0.04629	1.8	0.340	291.7±5.0	294±110	1
775_5.1	0.18	487	336	0.71	19.7	21.21	1.5	0.0523	2.1	0.0508	3.4	0.3300	3.7	0.04705	1.5	0.411	296.4±4.4	234±78	− 27
775_6.1	1.80	663	352	0.55	24.0	23.67	1.5	0.0745	1.6	0.0603	4.7	0.3450	5.0	0.04149	1.5	0.303	262.0±3.9	613±100	57
775_6.2	0.37	941	590	0.65	37.2	21.74	1.6	0.0522	1.5	0.0492	2.5	0.3107	3.0	0.04583	1.6	0.534	288.9±4.5	156±59	− 85
775_7.1	1.29	603	121	0.21	23.8	21.75	1.5	0.0647	1.7	0.0543	4.7	0.3400	4.9	0.04539	1.5	0.306	286.2±4.2	384±110	25
775_8.1	0.07	218	154	0.73	44.7	41.94	1.5	0.0948	1.1	0.0942	1.2	3.0930	1.9	0.23830	1.5	0.785	1378.0±19	1511±23	9
775_9.1	26.01	6847	10508	1.59	85.7	68.60	1.5	0.4660	0.8	0.3340	4.7	0.4970	5.7	0.01078	3.2	0.568	69.1±2.2	3638±71	98
775_10.1	0.87	224	95	0.44	9.2	21.01	1.7	0.0522	3.1	0.0452	7.4	0.2940	7.6	0.04717	1.7	0.227	297.1±5.0	− 46±180	744
775_10.2	0.00	378	241	0.66	16.0	20.35	1.6	0.0531	2.7	0.0531	2.7	0.3600	3.1	0.04915	1.6	0.509	309.3±4.7	335±60	8
775_11.1	0.69	157	78	0.52	6.4	21.09	1.9	0.0581	3.6	0.0526	4.7	0.3410	5.1	0.04709	1.9	0.366	296.6±5.4	310±110	4
775_12.1	0.27	625	284	0.47	25.8	20.80	1.5	0.0538	1.8	0.0516	2.7	0.3410	3.1	0.04794	1.5	0.484	301.8±4.4	269±61	− 12
775_12.2	0.07	973	643	0.68	39.6	21.13	1.5	0.0535	1.5	0.0529	1.6	0.3450	2.1	0.04730	1.5	0.680	297.9±4.2	325±36	8
775_13.1	1.08	103	43	0.42	4.2	21.07	2.1	0.0641	6.4	0.0554	11.0	0.3590	11.0	0.04695	2.1	0.197	295.7±6.1	430±240	31

Errors are 1-sigma; Pb_c and Pb^* indicate the common and radiogenic portions, respectively.
Error in Standard calibration was 0.49 % (not included in the above-mentioned errors but required when comparing data from different mounts).
(1) Common Pb corrected using measured ^{204}Pb.

Table 2c. SHRIMP data for rhyolite sample 776

Spot	$^{206}Pb_c$ %	U ppm	Th ppm	$^{232}Th/^{238}U$	$^{206}Pb^*$ ppm	Total $^{238}U/^{206}Pb$	±%	Total $^{207}Pb/^{206}Pb$	±%	(1) $^{207}Pb^*/^{206}Pb^*$	±%	(1) $^{207}Pb^*/^{235}U$	±%	(1) $^{206}Pb^*/^{238}U$	±%	Err. corr.	(1) $^{206}Pb–^{238}U$ age	(1) $^{207}Pb–^{206}Pb$ age	% Discord-ance
776_1.1	1.61	128	96	0.77	5.2	21.26	1.4	0.0566	4.1	0.0435	11.0	0.2780	12.0	0.046280	1.5	0.134	291.7±4.4	− 137±280	312
776_1.2	0.52	196	71	0.37	7.8	21.42	2.3	0.0523	4.1	0.0481	6.1	0.3080	6.5	0.046400	2.3	0.358	292.7±6.7	106±140	− 177
776_2.1	1.55	152	71	0.49	6.0	21.78	1.3	0.0604	3.6	0.0480	7.5	0.2990	7.6	0.045210	1.4	0.180	285.1±3.8	98±180	− 192
776_2.2	1.38	112	88	0.81	4.5	21.43	1.5	0.0619	4.1	0.0508	6.3	0.3220	6.5	0.046010	1.6	0.241	290.0±4.4	230±140	− 26
776_3.1	0.53	550	161	0.30	22.1	21.39	0.7	0.0534	2.0	0.0491	2.2	0.3146	2.3	0.046500	0.7	0.309	293.0±2.0	151±52	− 94
776_4.1	7.12	379	184	0.50	16.8	19.38	0.8	0.1619	1.7	0.1090	9.3	0.7190	9.4	0.047920	1.5	0.162	301.8±4.5	1779±170	83
776_4.2	0.37	637	351	0.57	25.5	21.45	0.8	0.0549	1.8	0.0519	2.9	0.3322	3.0	0.046450	0.8	0.259	292.7±2.2	279±65	− 5
776_5.1	0.09	579	419	0.75	23.0	21.65	0.7	0.0526	1.9	0.0519	2.0	0.3300	2.2	0.046150	0.7	0.329	290.9±2.0	279±47	− 4
776_6.1	0.58	325	133	0.42	13.0	21.48	0.9	0.0566	2.5	0.0520	4.9	0.3320	5.0	0.046280	1.0	0.191	291.6±2.7	284±110	− 3
776_7.1	0.18	855	657	0.79	34.2	21.47	0.6	0.0525	1.6	0.0511	2.2	0.3273	2.2	0.046490	0.6	0.271	292.9±1.7	244±50	− 20
776_8.1	1.71	100	70	0.72	4.2	20.48	1.6	0.0596	4.2	0.0458	14.0	0.3030	14.0	0.047990	1.7	0.125	302.1±5.2	− 15±340	2106
776_9.1	0.29	288	126	0.45	11.8	21.05	1.0	0.0550	3.0	0.0527	3.8	0.3440	4.0	0.047360	1.0	0.247	298.3±2.8	316±87	6
776_10.1	0.25	203	76	0.39	8.1	21.70	1.1	0.0587	3.1	0.0567	3.5	0.3590	3.6	0.045970	1.1	0.312	289.7±3.2	480±77	40
776_10.2	0.16	359	241	0.69	14.4	21.41	1.1	0.0569	2.3	0.0556	3.0	0.3570	3.2	0.046630	1.1	0.349	293.8±3.2	436±68	33
776_11.1	1.10	140	48	0.35	5.6	21.51	1.4	0.0578	5.3	0.0489	6.4	0.3100	6.6	0.045980	1.4	0.211	289.8±3.9	143±150	− 102
776_12.1	0.46	144	80	0.57	5.7	21.94	1.4	0.0574	3.8	0.0537	5.0	0.3360	5.1	0.045370	1.4	0.269	286.0±3.9	359±110	20

Errors are 1-sigma; Pb_c and Pb^* indicate the common and radiogenic portions, respectively.
Error in Standard calibration was 0.49 % (not included in the above-mentioned errors but required when comparing data from different mounts).
(1) Common Pb corrected using measured ^{204}Pb.

Table 2d. SHRIMP data for rhyolite sample 891

Spot	$^{206}Pb_c$ %	U ppm	Th ppm	$^{232}Th/$ ^{238}U	$^{206}Pb^*$ ppm	Total $^{238}U/$ ^{206}Pb	±%	Total $^{207}Pb/$ ^{206}Pb	±%	(1) $^{207}Pb^*/$ $^{206}Pb^*$	±%	(1) $^{207}Pb^*/$ ^{235}U	±%	(1) $^{206}Pb^*/$ ^{238}U	±%	Err. corr.	(1) $^{206}Pb–^{238}U$ age	(1) $^{207}Pb–^{206}Pb$ age	% Discord-ance
891_1.1	0.31	302	164	0.56	11.8	21.92	2.3	0.0565	2.6	0.0540	4.5	0.3390	5.1	0.04550	2.3	0.449	286.6±6.4	371±100	23
891_2.1	0.47	457	193	0.44	18.1	21.67	2.1	0.0537	2.1	0.0499	2.9	0.3160	3.6	0.04593	2.1	0.596	289.5±6.0	188±67	− 54
891_3.1	0.55	286	91	0.33	11.7	21.05	2.2	0.0549	4.2	0.0505	6.9	0.3290	7.2	0.04720	2.2	0.310	297.6±6.5	216±160	− 38
891_4.1	1.76	135	47	0.36	5.6	20.54	2.5	0.0663	3.5	0.0522	10.0	0.3440	11.0	0.04780	2.5	0.235	301.2±7.4	292±240	− 3
891_5.1	0.59	577	111	0.20	22.4	22.10	2.9	0.0519	2.0	0.0472	4.4	0.2920	5.3	0.04500	2.9	0.550	283.6±8.1	57±110	− 397
891_6.1	0.39	340	260	0.79	13.2	22.16	2.2	0.0539	4.1	0.0508	5.1	0.3150	5.5	0.04495	2.2	0.393	283.4±6.0	232±120	− 22
891_7.1	1.20	266	197	0.77	10.6	21.62	3.0	0.0632	2.7	0.0536	11.0	0.3380	11.0	0.04570	3.1	0.268	288.1±8.7	354±250	19
891_8.1	2.04	153	86	0.58	6.0	22.00	2.4	0.0581	4.6	0.0415	22.0	0.2550	22.0	0.04450	2.6	0.118	280.9±7.3	− 257±560	209
891_9.1	1.45	300	128	0.44	11.8	21.78	2.2	0.0588	2.8	0.0471	11.0	0.2940	11.0	0.04520	2.3	0.202	285.2±6.4	57±260	− 404
891_10.1	2.26	140	56	0.42	5.9	20.32	2.5	0.0736	8.4	0.0556	17.0	0.3690	17.0	0.04810	2.6	0.152	302.9±7.8	435±380	30
891_11.1	1.56	212	131	0.64	8.5	21.52	2.3	0.0588	4.0	0.0461	6.9	0.2910	7.3	0.04570	2.3	0.318	288.3±6.6	5±170	− 5293
891_12.1	0.29	747	372	0.51	28.3	22.69	2.1	0.0517	1.7	0.0494	3.0	0.2990	3.6	0.04393	2.1	0.569	277.2±5.6	165±70	− 68
891_13.1	1.86	135	85	0.65	5.4	21.64	2.6	0.0653	3.8	0.0503	13.0	0.3140	14.0	0.04540	2.7	0.200	285.9±7.7	207±310	− 38
891_14.1	0.73	150	88	0.61	5.8	22.10	2.6	0.0579	3.8	0.0521	10.0	0.3220	10.0	0.04490	2.6	0.255	283.3±7.3	288±230	2
891_15.1	1.68	173	55	0.33	7.0	21.09	2.4	0.0589	4.6	0.0453	14.0	0.2910	14.0	0.04660	2.5	0.180	293.7±7.2	− 42±330	801

Errors are 1-sigma; Pb_c and Pb^* indicate the common and radiogenic portions, respectively.
Error in Standard calibration was 0.49 % (not included in the above-mentioned errors but required when comparing data from different mounts).
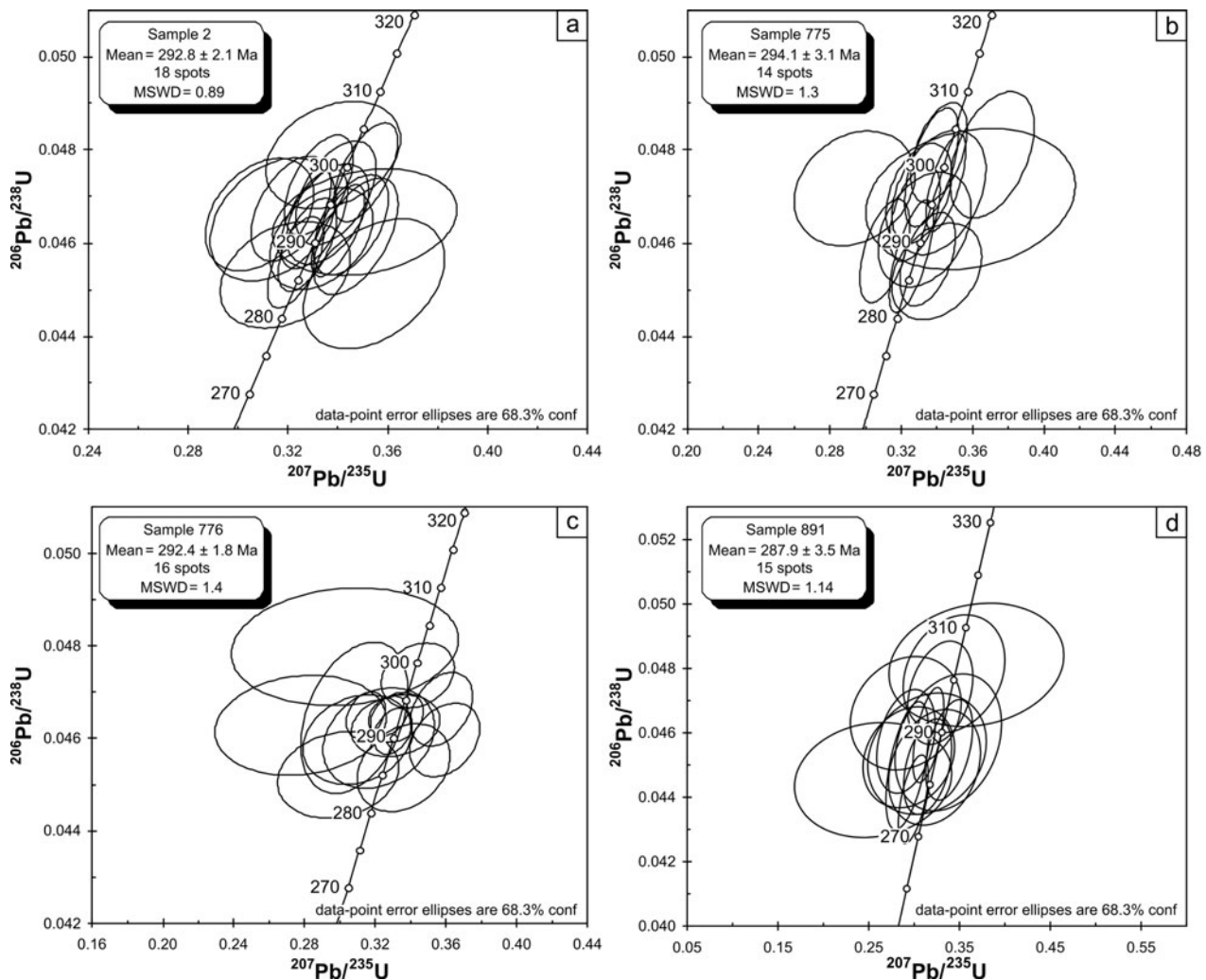(1) Common Pb corrected using measured ^{204}Pb.

Figure 4. Concordia diagrams for the samples dated. (a) Sample 2. (b) Sample 775. (c) Sample 776. (d) Sample 891.

of the entire group of 16 analyses is 292.4 ± 1.8 Ma (Fig. 4c). This corresponds to the Early Permian (Sakmarian) and is interpreted as the emplacement age of the Bolków Rhyolites.

4.c.4. Sample 891 (Sędziszowa rhyolite)

Fifteen spots in 15 crystals were analysed in sample 891. All the crystals represent a rather homogeneous population, mostly having relatively low U contents of 135–340 ppm (higher values of 450–750 ppm in three grains only) and $^{232}Th/^{238}U$ ratios ranging from *c.* 0.2 to 0.8. The $^{206}Pb_c$ is also usually below 1 %, but in seven grains slightly higher, reaching a maximum of 2.26 % in grain 10.1. The ages of all 15 grains fall in the range between 277 and 303 Ma, overlapping within errors. Three points display relatively high discordance (points 5.1, 9.1 and 11.1); their $^{206}Pb–^{238}U$ dates are relatively young (between 284 and 288 Ma), but overlap the mean age of the entire population: 287.9 ± 3.5 Ma (Fig. 4d; Early Permian – Artinskian). This age likely represents the emplacement and crystallization age of the Sędziszowa Rhyolites.

5. Discussion

5.a. The age of volcanism in the North-Sudetic Basin and constraints for basin evolution

The SHRIMP results point to the following emplacement ages of the silicic eruptive units of the in Lower Permian Volcanic Complex of the North-Sudetic Basin ($^{206}Pb–^{238}U$ ages, 1σ errors):

(1) Sędziszowa Rhyolites (sample 891) – 287.9 ± 3.5 Ma

(2) Bolków Rhyolites (sample 776) – 292.4 ± 1.8 Ma

(3) Wielisławka Rhyolites (sample 2) – 292.8 ± 2.1 Ma

(4) Różana Rhyolites (sample 775) – 294.1 ± 3.1 Ma

The ages of the Bolków, Wielisławka and Różana rhyolites – the major, most voluminous rhyolitic units in Lower Permian Volcanic Complex of the North-Sudetic Basin – are almost identical and indistinguishable within the analytical errors. These results constrain the age of the main stage of rhyolitic volcanism in the North-Sudetic Basin at *c.* 293 Ma. This age corresponds to the Early Permian – Sakmarian (ICS,

2012) and, considering the stratigraphic position of the Bolków and Różana rhyolites, confirms the assignment of the Wielisławka Formation to the Sakmarian (Wagner, 2008). Using the conventional SHRIMP technique with an error of *c.* ± 2 Ma, it is not possible to resolve whether the silicic volcanic units were emplaced in rapid succession, e.g. within thousands of years, or in more discrete episodes over a prolonged time period, e.g. of 1–2 Ma. However, the ages obtained, together with geological evidence, suggest that the Wielisławka Rhyolites (largely emplaced in basement rocks of the Stephanian–Autunian succession, in the central part of the basin) can be part of the feeder system for the Różana Rhyolites (lava flows in the overlying Autunian succession). In addition, the age obtained from the Sędziszowa Rhyolites is *c.* 5 Ma younger, only marginally overlaps the age of the adjacent Różana and Wielisławka rhyolites, and corresponds to the Artinskian. Thus, the Sędziszowa Rhyolites may reflect the youngest, volumetrically minor episode of rhyolitic (sub)volcanism in that area, resulting in the emplacement of a small dyke system.

The two stages of rhyolitic volcanism documented by our SHRIMP data are reminiscent of the 'two volcanic cycles' in the North-Sudetic Basin suggested by Kozłowski & Parachoniak (1967). However, the Wielisławka, Różana and Sędziszowa rhyolites of this study were in fact included into the same, 'second cycle', by these authors. Our data do not constrain directly the age of the mafic lavas of the Lower Permian Volcanic Complex of the North-Sudetic Basin. Field relationships, however, suggest that the majority of these mafic rocks were emplaced shortly after the rhyolites, partly as lava flows and partly as shallow-level sills/laccoliths in poorly lithified sediments (Awdankiewicz, 2006; Szczepara, 2012). Hoffmann *et al.* (2013) suggested that intermediate to basic volcanism at *c.* 296 Ma, characteristic of several late Variscan intramontane troughs in the Variscan orogen and especially voluminous in its northern foreland, may be linked to a regional switch from a convergent to a dextral strike-slip regime. It is possible, however, that the relative sequence and timing of silicic and mafic volcanism can also be influenced by local tectonic processes and/or evolution of individual magmatic systems.

The new data on the U–Pb ages of volcanism in the North-Sudetic Basin, together with the litho- and biostratigraphic evidence, put some general constraints on the timing of basin evolution. The onset of sedimentation in the basin, estimated at *c.* 303 Ma (Stephanian A–C), post-dates the metamorphism and deformation of the basement rocks by some 20 Ma. Volcanic activity followed the basin initiation by *c.* 10 Ma, at 294–292 Ma (the main stage of volcanism), with a minor subsequent stage at *c.* 287 Ma. This bimodal volcanism can be considered as a culmination of interrelated tectonic, volcanic and sedimentary processes and, at the same time, a termination of the early, rather short-lived but vigorous phase of basin development, strongly con-
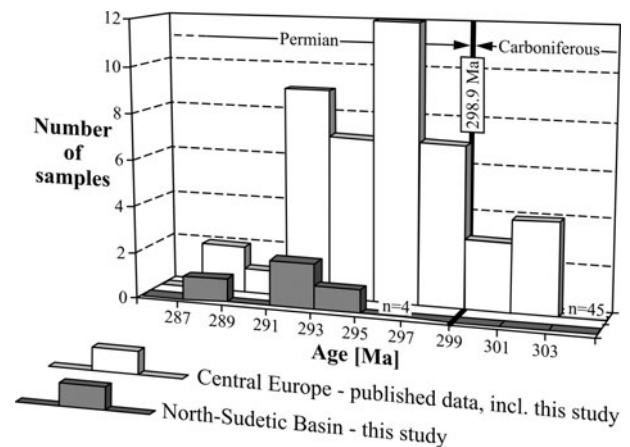

Figure 5. Comparison of the new SHRIMP ages of volcanic rocks from the North-Sudetic Basin with published ages for Stephanian–Permian volcanic rocks from Central Europe: the NE German Basin, the Polish Basin and several eruptive complexes of the Saxo-Thuringian Zone in southeastern Germany (data from: Breitkreuz & Kennedy, 1999; Breitkreuz *et al.* 2007; Nawrocki *et al.* 2008; Breitkreuz, Ehling & Sergeev, 2009; Hoffman *et al.* 2013).

trolled by tectonics (cf. Wojewoda & Mastalerz, 1989). This early phase was followed by a prolonged quiescence period of *c.* 30 Ma, documented by the hiatus above the Wielisławka Formation hosting the volcanic rocks. Continental sedimentation resumed at *c.* 260–250 Ma (Bolesławiec Formation), soon giving way to marine transgression (Zechstein deposits). Such a scenario is consistent with the waning of tectonic and magmatic activities in this part of the Variscan Belt during the Permian (McCann & Kiersnowski, 2008; Timmerman, 2008). The dating of post-magmatic minerals in the mafic lavas of the North-Sudetic Basin at *c.* 253 to 178 Ma (Pękala, Wójtowicz & Michalik, 2003) seems to reflect the crystallization of the secondary minerals after the burial of volcanic rocks by the younger deposits, in the course of diagenetic processes.

5.b. Regional correlations of volcanic and plutonic suites

In recent years, a number of U–Pb zircon (mostly SHRIMP) ages on the Permo-Carboniferous volcanic rocks of Central Europe were published (Breitkreuz & Kennedy, 1999; Breitkreuz *et al.* 2007; Nawrocki *et al.* 2008; Breitkreuz, Ehling & Sergeev, 2009; Hoffmann *et al.* 2013). A compilation of these results, together with our new data, is shown in Figure 5. Some of the eruptive units included in the compilation may be over-represented resulting in artefacts, e.g. the peak in the histogram at 291–293 Ma seems largely owing to several samples from the Halle Volcanic Complex (14 samples out of the total of 45). As found by Breitkreuz & Kennedy (1999) and supported by later data, the Late Palaeozoic volcanism spanned ('flared-up') across the boundary of Carboniferous and Permian. The compilation (Fig. 5) points to the regional climax of activity in the earliest Permian, between, broadly, 299 and 291 Ma; 78 % of samples dated fall in that age

range. The Permian volcanism in the North-Sudetic Basin may be correlated with relatively late phases of this volcanic climax. Ages between 291 and 295 Ma, corresponding to the main volcanic stage of the North-Sudetic Basin, are also reported from central Germany (e.g. from the Halle Volcanic Complex), and from the North-Saxon Volcanic Complex and the Döhlen Basin (Breitkreuz, Ehling & Sergeev, 2009; Hoffmann *et al*. 2013), as well as from some locations in the Polish Basin and the NE German Basin (drillings Daszewo-12, Wysoka Kamieńska-2, Salzwedel 2/64; Breitkreuz *et al*. 2007), and from the Kraków region (the Zalas laccolith; Nawrocki *et al*. 2008). On the other hand, preliminary SHRIMP results from the adjacent Intra-Sudetic Basin (Awdankiewicz & Kryza, 2012 and un-pub. data) suggest that the main stage of Permian volcanism in the latter basin occurred somewhat later, at *c*. 290 Ma. Thus, the timing of volcanism even in neigh-bouring late Variscan intramontane basins may not ne-cessarily have taken place coevally and, on the Central European scale, the spatial variation of ages of the up-permost Carboniferous / lower Permian volcanic rocks does not seem very systematic (cf. fig. 1 in Breitkreuz *et al*. 2007 and more recent data from Nawrocki *et al*. 2008; Breitkreuz, Ehling & Sergeev, 2009; Hoffman *et al*. 2013; this study).

The Variscan orogeny in the Sudetes was accom-panied, as elsewhere in the Variscan Belt, by in-tense and voluminous granitic plutonism. The Su-detic Late Palaeozoic granites have generally been subdivided into two age groups, *c*. 340–330 Ma and 320–300 Ma (Mazur *et al*. 2007), and new data show that the latest stages of this granitic magmatism ex-tended also into Permian times. The 294–292 Ma vol-canic rocks of the North-Sudetic Basin are broadly con-temporaneous with some granitoids east of the basin, e.g. in the Strzelin Massif, where the youngest and most voluminous plutonic phase is dated at *c*. 295 Ma (SHRIMP zircon ages; Oberc-Dziedzic, Kryza & Białek, 2010; Oberc-Dziedzic *et al*. 2013*b*). Compar-able ages of *c*. 298 Ma were also recently determined in the Strzegom-Sobótka Massif (SHRIMP results; Tur-niak, pers. comm., 2013). The broadly coeval Early Permian plutonic and volcanic events seem to be vari-ous expressions of, generally, the same magmatic pulse, related to the late Variscan, post-orogenic extension in the NE part of the Bohemian Massif (Kryza, Mazur & Oberc-Dziedzic, 2004; Mazur *et al*. 2006, 2007; McCann & Kiersnowski, 2008). Similar relationships are also recognized in neighbouring regions, e.g. in the Erzgebirge, where the youngest phases of granitic plutonism were contemporaneous with the basin form-ation and intrabasinal volcanism (Romer *et al*. 2012).

5.c. The origin of magma and the scarcity of inherited zircon

The voluminous Permian–Carboniferous magmatism in Europe was ultimately sourced in the mantle, as documented in the North-Sudetic Basin by the co-eval mafic volcanic rocks associated with the rhyolites (Awdankiewicz, 2006), by bimodal magmatic suites in other regions (e.g. the Oslo rift; Larsen *et al*. 2008), as well as the vast dolerite sill and dyke swarm com-plexes in the northern foreland of the Variscan orogen: in northern England, southern Sweden and in the North Sea (Heeremans *et al*. 2004; Timmerman, 2004; Tim-merman *et al*. 2009). The silica-rich volcanic rocks in Central Europe originated owing to differentiation of mantle-derived magmas at shallow lithospheric levels, with variable contribution of crustal components (e.g. Benek *et al*. 1996; Pietranik *et al*. 2013). A strong anatectic component in many Permian silica-rich vol-canic rocks is documented by abundant inherited zir-cons (e.g. Breitkreuz & Kennedy, 1999). In this context, a rather specific feature of the Permian rhyolites studied is the scarcity of such inherited zircon grains. Although our study was focused on dating the magmatic, hence young zircons, only a single analysis, out of 68 analysed spots in the four samples from the North-Sudetic Basin, represents a xenocrystic/inherited grain *c*. 1.4 Ga old (spot 8.1, sample 775). An overview of published SHRIMP data of the Stephanian–Autunian volcanic rocks in Central Europe (Breitkreuz & Kennedy, 1999; Breitkreuz *et al*. 2007; Breitkreuz, Ehling & Sergeev, 2009; Hoffman *et al*. 2013) shows that inherited zir-cons are not observed in 33 % of 44 samples analysed using the SHRIMP method. Thus, the scarcity of such zircons in several silicic volcanic units may be attrib-uted to: (1) the lack of significant crustal contribution in some of the rhyolitic magmas, (2) derivation or con-tribution from zircon-free crustal rocks, or (3) zircon elimination during crustal anatexis due to dissolution in Zr-undersaturated magma. It is difficult to decide what the reason was for the scarcity of inherited zircon in the rhyolites of the North-Sudetic Basin. This fea-ture is even more intriguing when we keep in mind that older zircons are much more abundant in the Variscan granitoids of similar age in this area. To solve these questions we would need more systematic analysis of these rocks, not only of their geochronology, but also of their petrology, geochemistry and isotopic charac-teristics.

6. Conclusions

(1) Three rhyolite samples representative of the main rhyolitic volcanic units from the Stephanian–Permian volcano-sedimentary succession of the North-Sudetic Basin yielded coherent SHRIMP zircon ages of *c*. 293 Ma that constrain the Early Permian – Sak-marian age of the rhyolitic volcanism in the eastern part of the Variscan Belt. The fourth sample, dated at 288 ± 4 Ma, represents a volumetrically minor, slightly younger stage of (sub)volcanic activity in Artinskian times. Mafic volcanism in this area shortly followed the eruption of felsic rocks.

(2) The new SHRIMP ages are coherent with the stratigraphic evidence and indicate that the bimodal volcanism terminated the early, short-lived

(*c*. 10–15 Ma) and vigorous stage of basin evolution. This volcanism correlates well with the late phases of the regionally developed main stage of Late Palaeozoic magmatism in Central Europe, constrained by previously published age data at 299–291 Ma. The Permian volcanism, together with coeval granitoid plutonism, can be linked to late Variscan, post-collisional extension.

References

ALEKSANDROWSKI, P., KRYZA, R., MAZUR, S. & ŻABA, J. 1997. Kinematic data on major Variscan strike-slip faults and shear zones in the Polish Sudetes, northeast Bohemian Massif. *Geological Magazine* **133**, 727–39.

AWDANKIEWICZ, M. 2006. Fractional crystallization, mafic replenishment and assimilation in crustal magma chambers: geochemical constraints from the Permian post-collisional intermediate-composition volcanic suite of the North-Sudetic Basin (SW Poland). *Geologia Sudetica* **38**, 39–61.

AWDANKIEWICZ, M., AWDANKIEWICZ, H., KRYZA, R. & RODIONOV, N. 2010*a*. SHRIMP zircon study of a micromonzodiorite dyke in the Karkonosze Granite, Sudetes (SW Poland): age constraints for late Variscan magmatism in Central Europe. *Geological Magazine* **147**, 77–85.

AWDANKIEWICZ, M. & KRYZA, R. 2012. Late-and post-orogenic volcanism in a Variscan intramontane trough: SHRIMP zircon ages, volume estimates and geodynamic significance of Permo-Carboniferous volcanic succession of the Intra-Sudetic Basin. *Mineralogia – Special Papers* **40**, 65–6.

AWDANKIEWICZ, M., PIECZONKA, J., PIESTRZYŃSKI, A. & SAWŁOWICZ, Z. 2010*b*. Late Palaeozoic post-orogenic volcanism in the Sudetes Mts. and Kupferschiefer-type ore deposits in the Fore-Sudetic Monocline, SW Poland. *Acta Universitatis Szegediensis. Acta Mineralogica – Petrographica, Field Guide Series* **18**, 2–34.

BARANOWSKI, Z., HAYDUKIEWICZ, A., KRYZA, R., LORENC, S., MUSZYŃSKI, A., DOLECKI, A. & URBANEK, Z. 1990. Outline of the geology of the Góry Kaczawskie (Sudetes, Poland). *Neues Jahrbuch für Geologie und Paläontologie, Abhandlungen* **179**, 223–57.

BENEK, R., KRAMER, W., MCCANN, T., SCHECK, M., NEGENDANK, F. J. W., KORICH, D., HUEBSHER, H.-D. & BAYER, U. 1996. Permo-Carboniferous magmatism of the Northeast German Basin. *Tectonophysics* **266**, 379–404.

BLACK, L. P., KAMO, S. L., ALLEN, C. M., ALEINIKOFF, J. N., DAVIS, D. W., KORSCH, R. J. & FOUDOULIS, C. 2003. TEMORA 1: a new zircon standard for Phanerozoic U–Pb geochronology. *Chemical Geology* **200**, 155–70.

BOSSOWSKI, A., SAWICKI, L. & WROŃSKI, J. 1981. *Mapa Geologiczna Polski 1:200 000. B – mapa bez utworów czwartorzędowych. Arkusz Wałbrzych*. Warszawa: Wydawnictwa Geologiczne (in Polish).

BREITKREUZ, C., EHLING, B.-C. & SERGEEV, S. 2009. Chronological evolution of an intrusive/extrusive system: the Late Paleozoic Halle Volcanic Complex in the north-eastern Saale Basin (Germany). *Zeitschrift der Deutschen Gesellschaft für Geowissenschaften* **160**, 173–90.

BREITKREUZ, C. & KENNEDY, A. 1999. Magmatic flare-up at the Carboniferous/Permian boundary in the NE German Basin revealed by SHRIMP zircon ages. *Tectonophysics* **302**, 307–26.

BREITKREUZ, C., KENNEDY, A., GEIßLER, M., EHLING, B.-C., KOPP, J., MUSZYNSKI, A., PROTAS, A. & STOUGE, S. 2007. Far eastern Avalonia: its chronostratigraphic structure revealed by SHRIMP zircon ages from Upper Carboniferous to Lower Permian volcanic rocks (drill cores from Germany, Poland and Denmark). *Geological Society of America Special Papers* **423**, 173–90.

CATHER, S. M., DUNBAR, N. W., MCDOWELL, F. W. & SCHOLLE, P. A. 2009. Climate forcing by iron fertilization from repeated ignimbrite eruptions: the icehouse–silicic large igneous province (SLIP) hypothesis. *Geosphere* **5**, 315–24.

FRĄCKIEWICZ, W. 1958. *Szczegółowa Mapa Geologiczna Sudetów 1:25 000. Arkusz Świerzawa*. Warszawa: Wydawnictwa Geologiczne (in Polish).

GEIßLER, M., BREITKREUZ, C. & KIERSNOWSKI, H. 2008. Late Paleozoic volcanism in the central part of the Southern Permian Basin (NE Germany, W Poland): facies distribution and volcano-topographic hiati. *International Journal of Earth Sciences (Geologische Rundschau)* **97**, 973–89.

GÓRECKA, T. 1970. Results of microfloristic research of Permo-Carboniferous deposits in the area between Jawor and Lubań. *Kwartalnik Geologiczny* **14**, 52–64 (in Polish, English summary).

GRAD, M., GUTERCH, A., MAZUR, S., KELLER, G. R., ŠPIČÁK, A., HRUBCOVÁ, P. & GEISSLER, W. H. 2008. Lithospheric structure of the Bohemian Massif and adjacent Variscan belt in central Europe based on profile S01 from the SUDETES 2003 experiment. *Journal of Geophysical Research* **113**, B10, doi: 10.1029/2007JB005497, 25 pp.

HEEREMANS, M., TIMMERMAN, M. J., KIRSTEIN, L. A. & FALEIDE, J. I. 2004. New constraints on the timing of the late Carboniferous – early Permian volcanism in the central North Sea. In *Permo-Carboniferous Rifting and Magmatism in Europe* (eds M. Wilson, E.-R. Neumann, G. R. Davies, M. J. Timmerman, M. Heeremans & B. T. Larsen), pp. 177–93. Geological Society of London, Special Publication no. 223.

HOFFMANN, U., BREITKREUZ, C., BREITER, K., SERGEEV, S., STANEK, K. & TICHOMIROWA, M. 2013. Carboniferous–Permian volcanic evolution in Central Europe—U/Pb ages of volcanic rocks in Saxony (Germany) and northern Bohemia (Czech Republic). *International Journal of Earth Sciences (Geologische Rundschau)* **102**, 73–99.

INTERNATIONAL COMMISSION ON STRATIGRAPHY. 2012. *International Chronostratigraphic Chart*. International Commission on Stratigraphy, August 2012. http://www.stratigraphy.org. Date last accessed: 30 October 2012.

JERZMAŃSKI, J. 1956. Porfir wzgórza Wielisławka w Górach Kaczawskich. *Przegląd Geologiczny* **4**, 174–5 (in Polish).

KOZŁOWSKI, S. & PARACHONIAK, W. 1967. Permian volcanism in the North-Sudetic depression. *Prace Muzeum Ziemi, Prace Petrograficzne i Geologiczne* **11**, 191–221 (in Polish, English summary).

KRYZA, R., CROWLEY, Q. G., LARIONOV, A., PIN, C., OBERC-DZIEDZIC, T. & MOCHNACKA, K. 2012. Chemical

abrasion applied to SHRIMP zircon geochronology: an example from the Variscan Karkonosze Granite (Sudetes, SW Poland). *Gondwana Research* **21**, 757–67.

KRYZA, R., MAZUR, S. & OBERC-DZIEDZIC, T. 2004. The Sudetic geological mosaic: insights into the root of the Variscan orogen. *Przegląd Geologiczny* **52**, 761–73.

KRYZA, R., WILLNER, A., MASSONNE, H.-J., MUSZYNSKI, A. & SCHERTL, H.-P. 2011. Blueschist-facies metamorphism in the Kaczawa Mountains (Sudetes, SW Poland) of the Central-European Variscides: P-T constraints by a jadeite-bearing metatrachyte. *Mineralogical Magazine* **75**, 241–63.

KRYZA, R. & ZALASIEWICZ, J. 2008. Records of Precambrian – Early Palaeozoic volcanic and sedimentary processes in the Central European Variscides: a review of SHRIMP zircon data from the Kaczawa succession (Sudetes, SW Poland). *Tectonophysics* **461**, 60–71.

LARSEN, B. T., OLAUSSEN, S., SUNDVOLL, B. & HEEREMANS, M. 2008. The Permo-Carboniferous Oslo Rift through six stages and 65 million years. *Episodes* **31**, 1–7.

LUDWIG, K. R. 2005*a*. *SQUID 1.12 A User's Manual. A Geochronological Toolkit for Microsoft Excel*. Berkeley Geochronology Center Special Publication, 22 pp.

LUDWIG, K. R. 2005*b*. *User's Manual for ISOPLOT/Ex 3.22. A Geochronological Toolkit for Microsoft Excel*. Berkeley Geochronology Center Special Publication, 71 pp.

MASTALERZ, K. 1990. Lacustrine successions in fault-bounded basins: 1. Upper Anthracosia Shale (Lower Permian) of the North-Sudetic Basin, SW Poland. *Annales Societatis Geologorum Poloniae* **60**, 75–106.

MAZUR, S., ALEKSANDROWSKI, P., KRYZA, R. & OBERC-DZIEDZIC, T. 2006. The Variscan Orogen in Poland. *Geological Quarterly* **50**, 89–118.

MAZUR, S., ALEKSANDROWSKI, P., TURNIAK, K. & AWDANKIEWICZ, M. 2007. Geology, tectonic evolution and Late Palaeozoic magmatism of Sudetes – an overview. In *Granitoids in Poland* (eds A. Kozłowski & J. Wiszniewska), pp 59–87. Archivum Mineralogiae Monograph no. 1.

MCCANN, T. & KIERSNOWSKI, H. (co-ordinators). 2008. Permian. In *The Geology of Central Europe. Vol. 1: Precambrian and Palaeozoic* (ed. T. McCann), pp. 531–98. London: The Geological Society of London.

MCCANN, T., PASCAL, C., TIMMERMAN, M. J., KRZYWIEC, P., LÓPEZ-GÓMEZ, J., WETZEL, A., KRAWCZYK, C. M., RIEKE, H., LAMARCHE, J. & SUNDVOLL, B. 2006. Post-Variscan (end Carboniferous – Early Permian) basin evolution in Western and Central Europe. In *European Lithosphere Dynamics* (eds D. G. Gee & R. A. Stephenson), pp 355–88. Geological Society of London, Memoirs no. 32.

MILEWICZ, J. 1965. Rotliegende deposits in the vicinity of Lwówek Śląski. *Biuletyn Instytutu Geologicznego* **185**. *Z badań geologicznych na Dolnym Śląsku* **11**, 195–228 (in Polish, English summary).

MILEWICZ, J. 1968. The geological structure of the north-sudetic depression. *Biuletyn Instytutu Geologicznego* **227**. *Z badań geologicznych na Dolnym Śląsku* **17**, 5–31 (in Polish, English summary).

MILEWICZ, J. & GÓRECKA, T. 1965. Preliminary remarks on the Carboniferous in the North-Sudetic depression. *Kwartalnik Geologiczny* **9**, 97–113 (in Polish, English summary).

MILEWICZ, J. & KOZDRÓJ, W. 1995. *Szczegółowa Mapa Geologiczna Sudetów 1:25 000. Arkusz Proboszczów*. Warszawa: Państwowy Instytut Geologiczny (in Polish).

MILEWICZ, J., SZAŁAMACHA, J. & SZAŁAMACHA, M. 1989. *Mapa Geologiczna Polski 1:200 000. B – Mapa bez Utworów Czwartorzędowych. Arkusz Jelenia Góra*. Warszawa: Wydawnictwa Geologiczne (in Polish).

NAWROCKI, J., FANNING, M., LEWANDOWSKA, A., POLECHOŃSKA, O. & WERNER, T. 2008. Palaeomagnetism and the age of the Cracow volcanic rocks (S Poland). *Geophysical Journal International* **174**, 475–88.

OBERC-DZIEDZIC, T. & KRYZA, R. 2012. Late stage Variscan magmatism in the Strzelin Massif (SW Poland): SHRIMP zircon ages of tonalite and Bt-Ms granite of the Gęsiniec intrusion. *Geological Quarterly* **56**, 225–36.

OBERC-DZIEDZIC, T., KRYZA, R. & BIAŁEK, J. 2010. Variscan multistage granitoid magmatism in Brunovistulicum: petrological and SHRIMP U-Pb zircon geochronological evidence from the southern part of the Strzelin Massif, SW Poland. *Geological Quarterly* **54**, 301–24.

OBERC-DZIEDZIC, T., KRYZA, R. & PIN, C. 2009. The crust beneath the Polish Sudetes: evidence from a gneiss xenolith in Tertiary basanite from Paszowice. *Geodinamica Acta* **22/3** 13−9.

OBERC-DZIEDZIC, T., KRYZA, R., PIN, C. & MADEJ, S. 2013*a*. Sequential granite emplacement: a structural study of the late-Variscan Strzelin intrusion, SW Poland. *International Journal of Earth Sciences* **102**, 1289–304.

OBERC-DZIEDZIC, T., KRYZA, R., PIN, C. & MADEJ, S. 2013*b*. Variscan granitoid plutonism in the Strzelin Massif (SW Poland): petrology and age of the Strzelin granites. *Geological Quarterly* **57**, 269–88.

OSTROMĘCKI, A. 1972. Tuffs and eruptive rock pebbles in the Upper Carboniferous near Świerzawa. *Geologia Sudetica* **6**, 315–21 (in Polish, English summary).

PAŃCZYK, M. & BACHLIŃSKI, R. 2004. Rb-Sr dating of Permian silica-rich volcanic rocks from the North-Sudetic Basin – preliminary data. *Mineralogia – Special Papers* **24**, 307–10.

PĘKALA, M., WÓJTOWICZ, A. & MICHALIK, M. 2003. Post-eruptive history of Lower Permian volcanic rock (trachybasalt from Lubiechowa; the North-Sudetic Basin). *Mineralogia – Special Papers* **23**, 145–7.

PERYT, T. 1978. Outline of the Zechstein stratigraphy in the North-Sudetic Trough. *Kwartalnik Geologiczny* **22**, 9–82.

PIETRANIK, A., SŁODCZYK, E., HAWKESWORTH, C. J., BREITKREUZ, C., STOREY, C. D., WHITEHOUSE, M. & MILKE, R. 2013. Heterogeneous zircon cargo in voluminous Late Paleozoic rhyolites: Hf, O isotope and Zr/Hf records of plutonic to volcanic magma evolution. *Journal of Petrology*. Published online 23 April 2013. doi: 10.1093/petrology/egt019.

ROMER, R. L., FÖRSTER, H.-J., KRONER, U., MÜLLER, A., RÖSSLER, R., RÖTZLER, J., SELTMANN, R. & WENZEL, T. (eds) 2012. *Granites of the Erzgebirge. Relation of Magmatism to the Metamorphic and Tectonic Evolution of the Variscan Orogen*. Guidebook to Eurogranites 2012 fieldtrip, October 7–13, 2012. Scientific Technical Report STR12/15. Helmholtz-Zentrum Potsdam – DeutschesGeoForschungsZentrum, 122 pp.

SCHECK-WENDEROTH, M. & LAMARCHE, J. 2005. Crustal memory and basin evolution in the Central European Basin System – new insights from a 3D structural model. *Tectonophysics* **397**, 143–65.

SKURZEWSKI, A. 1981. Permian volcanic rocks in the Bolków area. *Kwartalnik Geologiczny* **25**, 317–34 (in Polish, English summary).

STACEY, J. S. & KRAMERS, J. D. 1975. Approximation of terrestrial lead isotope evolution by a two-stage model. *Earth and Planetary Science Letters* **26**, 207–21.

STEIGER, R. H. & JÄGER, E. 1977. Subcommission on geochronology: convention on the use of decay constants

in geo- and cosmochronology. *Earth and Planetary Science Letters* **36**, 359–62.

SZCZEPARA, N. 2012. Permian bimodal volcanism in the North-Sudetic Basin: new insights into the emplacement processes, sequence and petrology of volcanic rocks of the Świerzawa area. *Mineralogia – Special Papers* **40**, 127–8.

SZCZEPARA, N. & AWDANKIEWICZ, M. 2010. Textural variation of Permian rhyolites of the North-Sudetic Basin. *Mineralogia – Special Papers* **37**, 110.

TIMMERMAN, M. J. 2004. Timing, geodynamic setting and character of Permo-Carboniferous magmatism in the foreland of the Variscan Orogen, NW Europe. In *Permo-Carboniferous Rifting and Magmatism in Europe* (eds M. Wilson, E.-R. Neumann, G. R. Davies, M. J. Timmerman, M. Heeremans & B. T. Larsen), pp. 41–74. Geological Society of London, Special Publication no. 223.

TIMMERMAN, M. J. 2008. Palaeozoic magmatism. In *The Geology of Central Europe. Vol. 1: Precambrian and Palaeozoic* (ed. T. McCann), pp. 665–48. London: The Geological Society of London.

TIMMERMAN, M. J., HEEREMANS, M., KIRSTEIN, L. A., LARSEN, B. T., SPENCER-DUNWORTH, E.-A. & SUNDVOLL, B. 2009. Linking changes in tectonic style with magmatism in northern Europe during the late Carboniferous to latest Permian. *Tectonophysics* **473**, 375–90.

TURNAU, E., ŻELAŹNIEWICZ, A. & FRANKE, W. 2002. Middle to early late Viséan onset of late orogenic sedimentation in the Intra-Sudetic Basin, West Sudetes: miospore evidence and tectonic implications. *Geologia Sudetica* **34**, 9–16.

WAGNER, R. (ed.) 2008. *Tabela Stratygraficzną Polski. Polska Pozakarpacka*. Warszawa: Ministerstwo Środowiska (in Polish).

WIEDENBECK, M., ALLÉ, P., CORFU, F., GRIFFIN, W. L., MEIER, M., OBERLI, F., Von QUADT, A., RODDICK, J. C. & SPIEGEL, W. 1995. Three natural zircon standards for U–Th–Pb, Lu–Hf, trace element and REE analyses. *Geostandards Newsletter* **19**, 1–23.

WILLIAMS, I. S. 1998. U–Th–Pb geochronology by ion microprobe. In *Applications in Microanalytical Techniques to Understanding Mineralizing Processes* (eds M. A. McKibben, W. C. Shanks III & W. I. Ridley), pp. 1–35. Reviews in Economic Geology vol. 7. Society of Economic Geologists.

WOJEWODA, J. & MASTALERZ, K. 1989. Climate evolution, allo- and autocyclity of sedimentation: an example from the Permo-Carboniferous continental deposits of the Sudetes. *Przegląd Geologiczny* **4**, 173–80 (in Polish, English summary).

ZIEGLER, P. A. & DEZES, P. 2006. Crustal evolution of Western and Central Europe. In *European Lithosphere Dynamics* (eds D. G. Gee & R. A. Stephenson), pp. 43–56. Geological Society of London, Memoirs no. 32.

ZIMMERMANN, E. & KÜHN, B. 1918. *Geologische Karte von Preussen und benachtbarten Deutschen Ländern, Blatt Schönau, Berlin* (in German).